Available at www.sciencedirect.com

INFORMATION PROCESSING IN AGRICULTURE 7 (2020) 93–108

journal homepage: www.elsevier.com/locate/inpa

Development and validation of an integrated mechatronic apparatus for measurement of friction coefficients of agricultural products

S.M. Shafaei [a], A. Nourmohamadi-Moghadami [a,*], S. Kamgar [a], M. Eghtesad [b]

[a] Department of Biosystems Engineering, School of Agriculture, Shiraz University, Shiraz 71441-65186, Iran
[b] Department of Solid Mechanics Engineering, School of Mechanical Engineering, Shiraz University, Shiraz 71348-51154, Iran

ARTICLE INFO

Article history:
Received 21 November 2018
Received in revised form
16 March 2019
Accepted 19 April 2019
Available online 25 April 2019

Keywords:
Static friction coefficient
Dynamic friction coefficient
Physical property
Friction force

ABSTRACT

An integrated mechatronic apparatus was developed based on tilting plate method in order to precisely measure static friction coefficient (SFC) and dynamic friction coefficient (DFC) of agricultural products. The apparatus consisted of two main parts (mechanical and electrical parts). The main element of mechanical part was rotary container. Meanwhile, the electrical part included control, display, goniometer, level controller, rotational power supply, and infrared unit. The apparatus was initially simulated in simulation environment and practically calibrated to achieve high precision measurements. To appraise performance of the apparatus, the SFC and DFC of three grains were measured on five contact surfaces. Experiments were also conducted by means of a typical apparatus operating based on puling force method. Some statistical descriptor parameters such as mean absolute percentage error (MAPE), average of absolute values of measurement errors (AAVME), maximum of absolute values of measurement errors (MAVME), and correlation coefficient were used to compare accuracy of the apparatus with the typical one. The acceptable AAVME (<10%), MAVME (<10%), MAPE (<5%), and correlation coefficient (>0.9) indicated high accuracy, stability, and efficiency of the apparatus for automatic measurements of the SFC and DFC. From practical point of view, the mechatronic apparatus would be a beneficial tool for experimental, educational, demonstrational, and research works.

1. Introduction

Physical properties of agricultural products are needed for designing of planting, harvesting, and post-harvest handling/processing machinery and equipment. Some important physical properties are known as major dimensions (length, width, and thickness), geometric mean diameter, mass, sphericity, and friction coefficients. The friction coefficient is key parameter required to determine loads produced by

* Corresponding author.
E-mail address: a.nourmohamadi@shirazu.ac.ir (A. Nourmohamadi-Moghadami).

Peer review under responsibility of China Agricultural University.

Abbreviations: AAVME, average of absolute values of measurement errors; DFC, dynamic friction coefficient; LCD, liquid-crystal display; MAPE, mean absolute percentage error; MAVME, maximum of absolute values of measurement errors; PATA, parallel advanced technology attachment; PID, proportional-integral-derivative; SFC, static friction coefficient

https://doi.org/10.1016/j.inpa.2019.04.006
2214-3173

Nomenclature

a	acceleration (cm/s^2)
B	bulk density of stored product (kg/m^3)
CV	coefficient of variation (%)
D_g	geometric mean diameter (mm)
F_k	dynamic frictional force (N)
F_s	static frictional force (N)
F_x	force in direction X (N)
F_y	force in direction Y (N)
FC_i	ith friction coefficient
$FC_{meas,i}$	ith friction coefficient measured by tilting plate method based apparatus
$FC_{ind,i}$	ith friction coefficient indicated by pulling force method based apparatus
g	gravity acceleration (m/s^2)
G	gravity constant (9.8×10^{-3} kN/kg)
H	hydraulic radius of the bin (m)
k	ratio of lateral to vertical pressure
L	length (mm)
L(Y)	lateral pressure of product at depth Y (kPa)
M	mean of friction coefficient
m	product mass (g)
MAPE	mean absolute percentage error (%)
N	normal force (N)
n	number of data
R	correlation coefficient
S	sphericity (%)
S_a	surface area (mm^2)
SD	standard deviation
T	thickness (mm)
t	time (s)
t_1	time at the first position on inclined plane (s)
v	sliding velocity (cm/s)
v_1	sliding velocity at the first position on inclined plane (cm/s)
v_2	sliding velocity at the second position on inclined plane (cm/s)
V(Y)	vertical pressure of product at depth Y (kPa)
W	width (mm)
x	distance (cm)
Y	equivalent product depth (m)
μ	friction coefficient of product on structural surface
μ_s	static friction coefficient
μ_k	dynamic friction coefficient
θ	inclined plane angle (°)
Δt_1	time required for body movement from the first to the second position on inclined plane (s)
Δt_2	time required for body movement from the second to third position on inclined plane (s)
Δx_1	distance between the first and second position on inclined plane (cm)
Δx_2	distance between the second and third position on inclined plane (cm)

product pressures on storage bin walls and hopper surfaces, based on the following Eqs. (1) and (2) [1].

$$V(Y) = \frac{BHG}{\mu k}\left[1 - \exp\left(\frac{-\mu kY}{H}\right)\right] \quad (1)$$

$$L(Y) = kV(Y) \quad (2)$$

Friction coefficients are classified as the SFC and DFC. The SFC affects friction force for initial movement of a body, while the DFC affects dynamic friction force. Hence, accurate measurement of the SFC and DFC of agricultural products is of great importance.

Numerous researches accomplished earlier have reported that the SFC and DFC depend strongly on precision of measuring method. Thus, to accurately measure the SFC and DFC of specific product by taking several considerations into account, various apparatuses have been developed based on three measuring methods named pulling force, tilting plate, and rotating disk. According to these methods, some published papers for development of the SFC and DFC measuring apparatus are chronologically provided in Tables 1 and 2, respectively.

Pulling force method was originally initiated based on friction force measurement. The SFC and DFC are then obtained from relationship between friction force and experimental mass. In case of rotating disk method, it was established on the basis of torque required for rotation of carrier disk. However, calculation of the SFC and DFC is independent of experimental mass for tilting plate method. The following paragraphs describe advantages and disadvantages of each method, as well as challenges which are faced.

As it can be seen in the Tables 1 and 2, pulling force method was used more than two other methods, since pulling force based apparatus could measure both the SFC and DFC. However, this apparatus need different devices with data acquisition system like universal tensile/compression testing machine.

Study of published papers cited in Table 2 indicated that the DFC was determined using apparatus fabricated on the basis of both pulling force and rotating disk methods. However, portability of the apparatus reduced because several external devices used to command and control the apparatus. Moreover, some apparatuses developed for measuring the DFC of specific products were not usable for other products in different situations. Therefore, it is favorable to develop a DFC measuring apparatus with portable devices applicable for every product.

According to the Tables 1 and 2, pulling force and rotating disk methods were frequently used to measure the SFC and DFC, but tilting plate method was only used for determination of the SFC. Although tilting plate method can only use to determine the SFC, simple structure of such apparatuses is highlight. Also, this apparatus was usually developed for specific products.

Table 1 – Developed SFC measuring apparatuses for some agricultural products.

Measuring method	Experimental product	Authors	Year
Pulling force			
	Sweet potato	Fluck et al. [2]	1968
	Sorghum	Stewart et al. [3]	1969
	Potato	Schaper and Yaeger [4]	1992
	Watermelon	Puchalski and Brusewitz [5]	1996
	Wheat	Molenda et al. [6]	2000
	McLemore and Gala apples	Puchalski and Brusewitz [7]	2001
	Wheat	Molenda et al. [8]	2002
	Apple	Puchalski et al. [9]	2002
	Orange and sweet lemon	Singh et al. [10]	2004
	Kidney bean, dry pea and black-eyed pea	Altuntas and Demirtola [11]	2007
	Rapeseed	Rusinek and Molenda [12]	2007
	Wheat and faba bean	Sharobeem [13]	2007
	Millet grains and flours	Subramanian and Viswanathan [14]	2007
	Grapefruit (*Citrus paradisi*)	Ince and Vursavus [15]	2008
	Sorghum and millet	Nwakonobi and Onwualu [16]	2009
	Tomato	Li et al. [17]	2011
	Paddy	Alizadeh and Minaei [18]	2012
	Soybean	LoCurto et al. [19]	2014
	Dried distillers grains	Nyendu et al. [20]	2014
Tilting plate			
	Cumin	Singh and Goswami [21]	1996
	Wheat	Molenda et al. [6]	2000
	Green gram	Nimkar and Chattopadhyay [22]	2001
	Wheat	Molenda et al. [8]	2002
	Wheat	Tabatabaeefar [23]	2003
	Cowpea, maize and groundnut	Bart-Plange et al. [24]	2007
	Wheat	Lorestani et al. [25]	2012
	Wheat, rye, barley, oats and triticale	Kaliniewicz [26]	2013
	Soybean	LoCurto et al. [19]	2014
	Wheat, barley, chickpea, safflower, soybean, rye and sunflower seed	Shafaei et al. [27]	2015
	Wheat, rye, barley, oats and triticale seed	Kaliniewicz et al. [28]	2016
Rotating disk			
	Soybeans, red kidney beans and unshelled peanuts	Chung and Verma [29]	1989
	Alfalfa	Shinners et al. [30]	1991
	Sunflower seed and its kernel	Gupta and Das [31]	1998

Published studies mentioned in the Tables 1 and 2 demonstrated that researchers preferred to use a measuring apparatus with simple structure, similar to tilting plate method based apparatus, and ability to determine both the SFC and DFC. Hence, it is desirable to develop a measuring apparatus capable to precisely measure both the SFC and DFC of agricultural products without immobile elements. A review of the literature summarized in the Tables 1 and 2 indicated that there have been no published attempts for automation and development of general tilting plate method based apparatus for measurement of the SFC and DFC of agricultural products. Accordingly, the aims of this research were concentrated on the below items:

(a) Development, calibration, and validation of a mechatronic portable measuring apparatus which was designed based on tilting plate method to exactly determine the SFC of agricultural products.
(b) To extend capability of the developed SFC measuring apparatus to exactly determine the DFC of agricultural products at different sliding velocities, based on tilting plate method.

2. Materials and methods

2.1. Theoretical background

2.1.1. SFC

All forces acting on an unmoving object on inclined plate are shown in Fig. 1. To balance forces in the Cartesian coordinate system (X and Y coordinates), the following equations are extracted.

Table 2 – Developed DFC measuring apparatuses for some agricultural products.

Measuring method	Experimental product	Authors	Year
Rotating disk			
	Wheat	Henderson [32]	1967
	Rapeseed, vetch, millet	Rademacher [33]	1978
	Wheat and barley	Lawton [34]	1980
	Soybeans and shelled corn	Tsang-Mui-Chung et al. [35]	1984
	Soybeans, red kidney beans and unshelled peanuts	Chung and Verma [29]	1989
	Alfalfa	Shinners et al. [30]	1991
	Sunflower seed and its kernel	Gupta and Das [31]	1998
	Paddy	Asli-Ardeh et al. [36]	2010
Pulling force			
	Barley and shelled corn	Bickert and Buelow [37]	1966
	Wheat	Snyder et al. [38]	1967
	Sweet potato	Fluck et al. [2]	1968
	Sorghum	Stewart et al. [3]	1969
	Cotton seed	Clark et al. [39]	1970
	Orange	Chen and Squire [40]	1971
	Corn, soybeans and chicken feed	Clark and McFarland [41]	1973
	Wheat	Thompson and Ross [42]	1983
	Wheat	Moore et al. [43]	1984
	Wheat, flaxseed, lentil and faba bean	Irvine et al. [44]	1992
	Potato	Schaper and Yaeger [4]	1992
	Wheat	Bucklin et al. [45]	1996
	Watermelon	Puchalski and Brusewitz [5]	1996
	Wheat	Molenda et al. [6]	2000
	McLemore and Gala apples	Puchalski and Brusewitz [7]	2001
	Chickpea	Tavakoli et al. [46]	2002
	Rice	Mingjin et al. [47]	2003
	Orange and sweet lemon	Singh et al. [10]	2004
	Kidney bean, dry pea and black-eyed pea	Altuntas and Demirtola [11]	2007
	Wheat and faba bean	Sharobeem [13]	2007
	Mixture of corn grits and peanut flour, corn flour, corn grits and rice grits	Ghonimy [48]	2007
	Yellow corn grits, wheat bran, soybean meal and cotton seed meal	Ibrahim [49]	2008
	Grapefruit (*Citrus paradisi*)	Ince and Vursavus [15]	2008
	Wheat	Asli-Ardeh et al. [50]	2017
	Wheat	Schwab [51]	2017

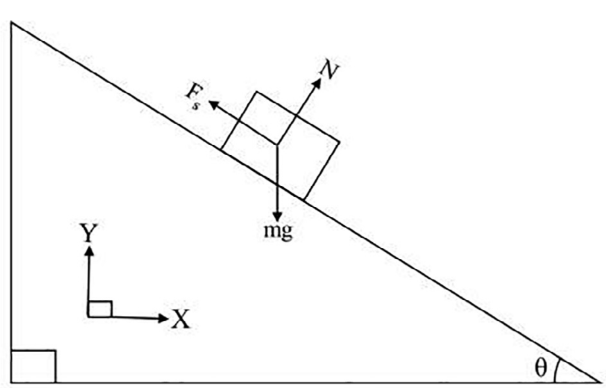

Fig. 1 – Free body diagram of an unmoving object on inclined plate.

$$\sum F_x = mg\sin\theta - F_s = 0 \quad (3)$$

$$\sum F_y = mg\cos\theta - N = 0 \quad (4)$$

In sliding threshold of object on inclined plate, needed pulling force is equal to maximum static friction force existing between two contact surfaces. Static friction force is function of the SFC and normal force (Eq. (5)).

$$F_s = \mu_s N \quad (5)$$

Combination of the Eqs. (3)–(5) results in a mathematical relationship between the SFC and geometric properties of inclined plate for threshold of object slide on inclined plate. The Eq. (6) describes this relationship.

$$\mu_s = \tan\theta \quad (6)$$

2.1.2. DFC

Applying the Newton's second law for inclined plate in X and Y direction (Fig. 2) results in the following equations.

$$\sum F_x = mg\sin\theta - F_k = ma \quad (7)$$

$$\sum F_y = mg\cos\theta - N = 0 \quad (8)$$

Relation between frictional and normal force applied on a body is described by term of the DFC (μ_k) as:

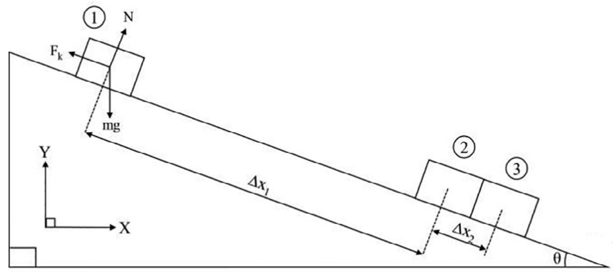

Fig. 2 – Free body diagram of a moving object on the first, second, and third position on inclined plate.

$$F_k = \mu_k N \tag{9}$$

The Eqs. (7)–(9) can be combined as:

$$\mathrm{mg}\sin\theta - \mu_k \mathrm{mg}\cos\theta = \mathrm{ma} \tag{10}$$

There is no information about body motion (constant, linear, or nonlinear acceleration) over distance between the first and second position of body on inclined plane. However, mathematical definition of acceleration can be used as the following Eq. (11).

$$a = \frac{dv}{dt} \tag{11}$$

With substituting the Eq. (11) in the Eq. (10) and rearranging the Eq. (10), the Eq. (12) is obtained.

$$(\tan\theta - \mu_k)dt = \frac{dv}{g\cos\theta} \tag{12}$$

By integrating the Eq. (12) over distance between the first and second position of body on inclined plane and considering initial conditions as $v_1 = 0$ and $t_1 = 0$, the Eq. (13) is obtained.

$$\mu_k = \tan\theta - \frac{v_2}{\Delta t_1 g\cos\theta} \tag{13}$$

Since the second and third positions are very close together and distance between them is negligible compared to that of the first and second positions ($\Delta x_1 > \Delta x_2$), sliding velocity between the second and third positions is assumed to be constant (Eq. (14)). Therefore, the Eq. (13) can be rewritten as the Eq. (15).

$$\Delta x_2 = v_2 \Delta t_2 \tag{14}$$

$$\mu_k = \tan\theta - \frac{\Delta x_2}{\Delta t_2 \Delta t_1 g\cos\theta} \tag{15}$$

2.2. *Designing of apparatus*

2.2.1. *SFC measuring*

According to the Section 2.1.1, the SFC measuring system had to detect inclined plate angle in threshold of object slide and calculate the SFC using the Eq. (6). To achieve the accurate SFC, it is necessary to know exact angle of inclined plate in sliding threshold. Thus, the system should be worked through increment of inclined plate angle from zero to desired angle.

2.2.2. *DFC measuring*

According to the Eq. (15), the DFC can be measured in specific angle of inclined plate. Slop angle of the plate is fixed. Distance between the first and second positions is chosen by operator and distance between the second and third positions is fixed ($\Delta x_2 = 0.5$ cm). Object is released from the first position. As influenced by gravity, body straightly moves from the first position to the second and the third positions through distances of Δx_1 and Δx_2, respectively. Time required for straight movement of object between two distances is accurately measured and used to calculate the DFC based on the Eq. (15). Consequently, sliding velocity of body on the second position can be calculated using the Eq. (14).

2.3. *Apparatus development*

The apparatus consisted of two main parts, mechanical and electrical parts. Mechanical part comprised chassis, driven shaft, mechanical joints, and an inclined plate (rotary container). Taking engineering principles into consideration, hard wood, steel, and aluminum were hired for chassis, driven shaft, and rotary container, respectively. Plywood, galvanized steel, rubber, glass, and aluminum plates were selected as experimental surfaces. All parts of the apparatus were mounted on chassis and the container was installed on driven shaft. The electrical part included control, display, goniometer, level controller, rotational power supply, and infrared unit. Fig. 3 shows block diagram of the apparatus units. These electrical units were integrated in order to handle measuring procedure automatically. Components of each electrical unit were chosen based on the highest operational resolution and working cycle, reasonable cost, capability of provision, and ease of use. Fundamental tasks of each electrical unit are described in detail by the following subsets.

2.3.1. *Rotational power supply*

A commercial direct current gear motor (model: 9ZGA60FM-G, manufacture: ZHENG, made in China) with reduction ratio of 1/334 was utilized to convert controlled electrical power into rotational mechanical power. The motor shaft was coupled with a driven shaft by some mechanical joints. On the other hand, rotary container, which was aligned with driven shaft, simultaneously rotated by revolution of the motor shaft. Constant rotational speed of the motor (0.25 rpm) was defined by control unit according to predetermined considerations. These considerations were taken to keep the motor shaft under control with an angular accuracy of ±1°. Before practical trials, to adjust rotary container slop, rotation direction of the motor shaft was manually altered by operator as clockwise or counterclockwise.

2.3.2. *Control unit*

The control unit was main part of the apparatus. The unit comprised an AVR-Atmega 8 microcontroller, made by the ATMEL Corporation, as its core. The unit could adapt 220 V to desired voltage for each electrical element. By sending proper commands to the motor and LCD element, the unit controlled automatic measuring process. Logical calculations were performed by the unit, in order to extract the SFC and DFC based on formula registered in its memory. In accordance with the Eqs. (6) and (15), the formula was defined in CodeVision simulator software for optimum performance of the

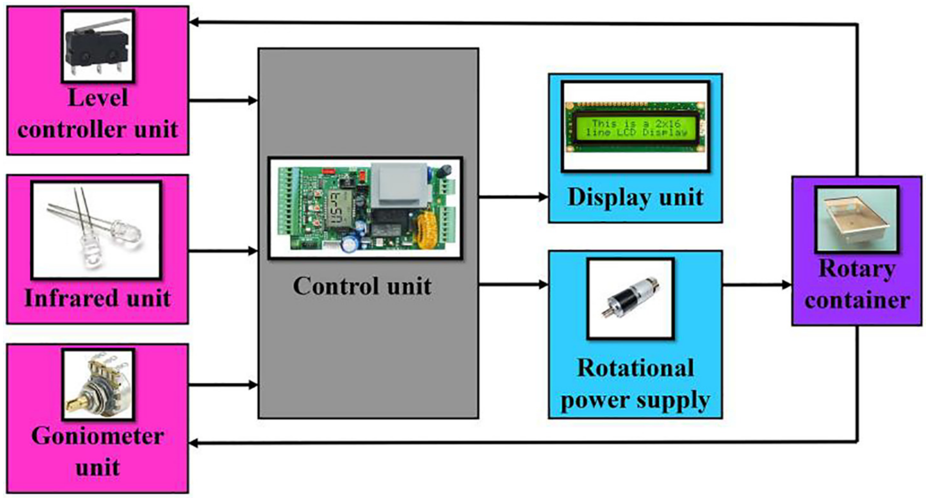

Fig. 3 – Block diagram of the apparatus units.

unit core. The PID controller method was used in the control unit circuit to control the aforementioned tasks.

2.3.3. *Goniometer unit*

To exactly sense rotational movement of driven shaft, a variable rate resistor, known as potentiometer (model: B5K-20 mm, made by Jahan electronic industrial company, Iran), was attached to the driven shaft. A voltage (0–5 V) was sent from the resistor to the control unit based on changes of rotational angle of the driven shaft. Linear relationship was assigned between rotational angle of the driven shaft and output voltage. The control unit continuously converted the received voltage values to the angle values, based on specified linear relationship.

2.3.4. *Infrared unit*

Position of sliding body on rotary container was determined using a pair of infrared sensors. The pair consisted of an infrared emitter and a detector. The infrared light was sent out by the emitter (model: LD271, manufacture: Osram, made in Malaysia) and received by the detector (model: BPV10, manufacture: Vishay, made in Malaysia) in case of in-line opposite position of the sensors. Moving through container, object cut the infrared light between emitter and detector off. Partial movement of sliding body could be detected by disconnection between the sensors. The infrared connection between the sensors was always checked by the control unit. The infrared sensors were placed into a graded groove created on two sides of the container based on size of experimental product.

2.3.5. *Display unit*

Rotation angle of the container, error messages, and the SFC and DFC were displayed on the LCD of the display unit. The unit circuit was connected to the control unit through the PATA cable. The PATA cable can transfer data in parallel form without disturbance and time delay.

2.3.6. *Level controller unit*

Rotation angle of the container was limited between 0 and 90 degrees using two micro switches (model: 1185RE8, made by Omron company, Japan). To prevent damage to the apparatus due to excessive rotation of the container (both clockwise and counterclockwise rotations), two micro switches were installed in appropriate locations. As the container came into contact with each micro switch, electrical power of the motor was instantly stopped by the control unit. In this situation, the container was placed in -1° or 91° with respect to based level.

2.4. *Measuring procedure*

2.4.1. *SFC*

Zero-degree angle of the container was adjusted by the system operator utilizing electrical switches of the control unit of the apparatus. To reach zero angle, the control unit continuously computed the container angle value during rotation and displayed it on the LCD. Angle control process was carried out between 0 and 90 degrees. Error message was appeared on the LCD, when angle exceeded defined range. The control unit constantly checked the infrared light between the emitter and detector paired sensors. This method was applied in order to detect opposite position of the emitter and detector. If correct location of the infrared paired sensors was not detected, an error message was then displayed on the LCD. A closed-loop control of the container angle and desired position of the sensors were repeated to achieve desirable conditions. Finally, the message, “SFC measuring apparatus is ready to use”, was displayed on the LCD, when zero-degree angle of the container and proper in-line situation of the infrared sensors were achieved.

Sliding object was placed on the container behind two infrared paired sensors. The container angle increased with accuracy of 1°. Exact angle of the container was continuously displayed on the LCD and recorded on memory of the control unit. During increment of the container angle, the control unit regularly checked connection between the infrared emitter and detector sensors. In specific angle of the container, since the gravity force exceeded maximum frictional force, object released and connection between two infrared paired sensors was disconnected. In order to prevent angle increment of the container, the control unit rapidly stopped the

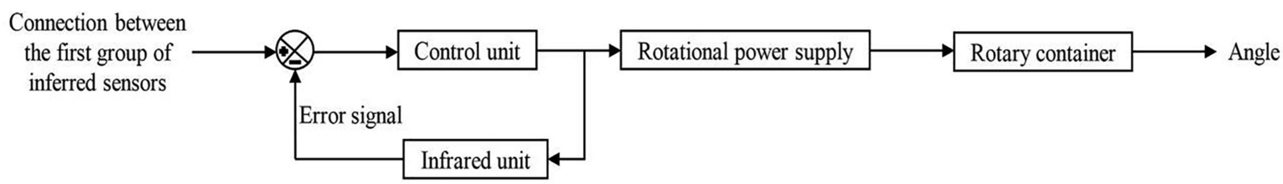

Fig. 4 – Block diagram of closed-loop control system of the PID controller for the SFC measuring procedure.

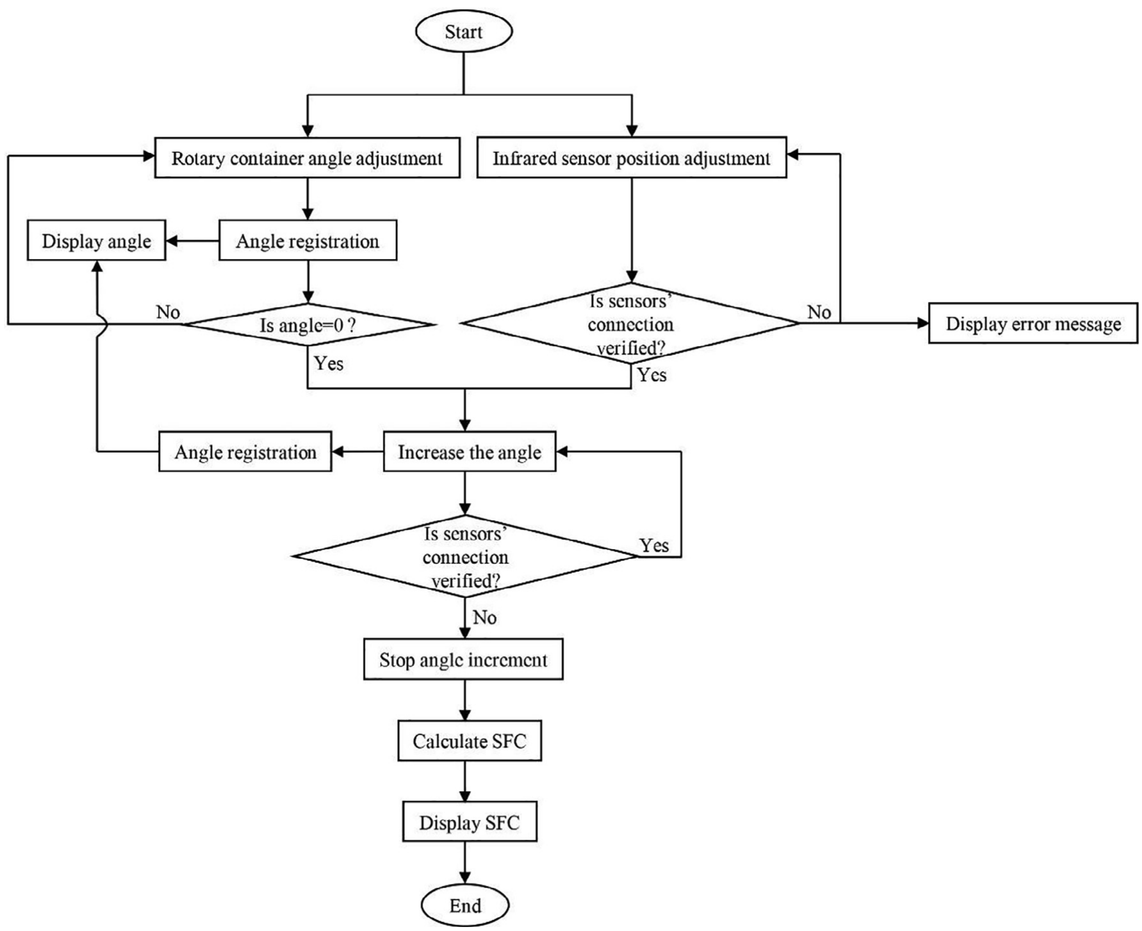

Fig. 5 – Operational flowchart of the SFC measuring system.

motor and calculated the SFC using the last recorded angle of the container and the Eq. (6) simultaneously. As a final point of the procedure, the calculated SFC was displayed on the LCD. Fig. 4 depicts block diagram of the closed-loop control system of the PID controller for the SFC measuring procedure. The Fig. 4 shows how the units operate simultaneously in order to control measuring procedure of the SFC. The operational flowchart of the SFC measuring system is also shown in Fig. 5.

2.4.2. DFC

The container angle was adjusted by operator using electrical switches of the control unit of the apparatus. The control unit continuously computed the container angle value and displayed it on the LCD. The control process was carried out between 0 and 90 degrees. The error message was appeared on the LCD, when the angle exceeded the defined range. The last adjusted angle value was registered on processor memory of the control unit. It was not altered until the container angle was changed. The control unit unendingly tracked connection between two infrared emitter and detector sensors for the first, second, and third group of the paired sensors. This method was applied in order to detect the emitter and detector against each other. If correct location of two infrared sensors of a group was not detected to be against each other, the LCD displayed an error message. A closed loop control of the container angle and inline position of the infrared paired sensors repeated to achieve desired condition. Finally, the message, “DFC measuring apparatus is ready to use”, was displayed on the LCD.

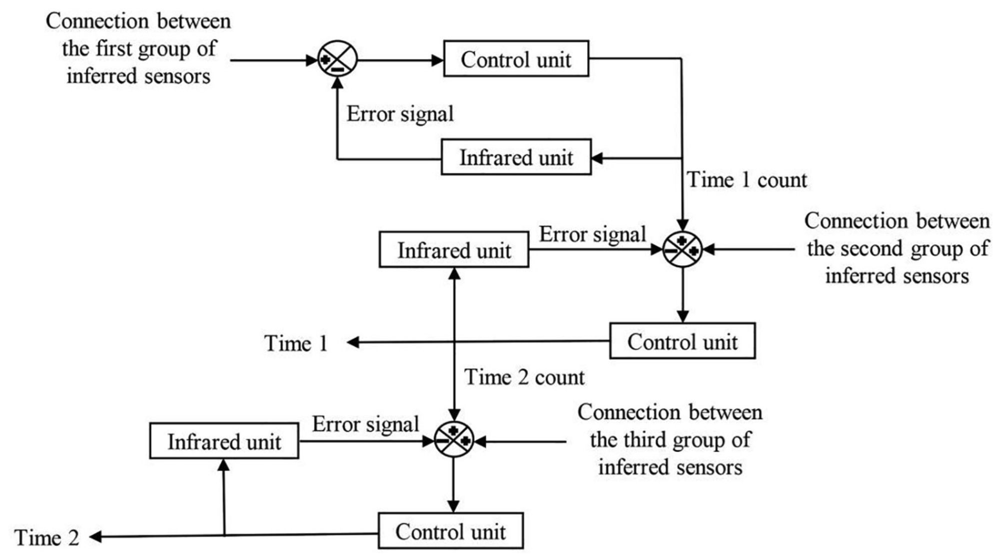

Fig. 6 – Block diagram of closed-loop control system of the PID controller for the DFC measuring procedure.

Sliding object was placed on a position before the first group of the infrared paired sensors. Once the object was released, it disconnected connection between two infrared paired sensors and the control unit started to count time (Δt_1). The time was continuously displayed on the LCD. As object reached to the second group of infrared paired sensors, time count was momentarily stopped and the time was recorded on the main microcontroller memory of the control unit. Then, the control unit rapidly started to count time (Δt_2). In this situation, object was between the second and third group of paired infrared sensors. The time count was stopped and saved in the microcontroller memory of the control unit, when object reached to the third paired infrared sensors. The control unit calculated the DFC and sliding velocity in position of the second paired infrared sensors using measured times, angle, and distance values recorded on its memory ($\Delta x_2 = 0.5$ cm), by means of the Eqs. (15) and (14), respectively. As a final point of the procedure, the determined DFC and sliding velocity could be observed on the LCD. Fig. 6 depicts block diagram of the closed-loop control system of the PID controller for the DFC measuring procedure. The Fig. 6 shows how the units operate simultaneously in order to control measuring procedure of the DFC. The operational flowchart of the DFC measuring system is also shown in Fig. 7. Note that, changing angle of the container and Δx_1 led to achievement of desired sliding velocity of object in the second position.

2.5. *Laboratory simulation*

Operations of breadboard version of initial balance prototype of the electrical units were simulated in electrical measurement laboratory using portable laptop computer and frequency function generator. Main goal of simulation was to check accuracy of the electrical elements and units in five areas, including sensitivity, damping, stability, shock and vibration, and transient response. To reduce operator errors, each simulation procedure was performed in three replications with the same settings.

2.6. *Calibration and data delimitation*

Comprehensive calibration trails were carried out to determine measurement linearity between observed and calculated values obtained from the container angle. An angle measuring instrument named protractor, with precision of ±1°, was installed on the driven shaft to compare calculated and observed angle values of the container. Every angle (0–90) of the container was measured using both methods (goniometer unit and installed protractor). To reduce error, the trails were completed three times and mean values were used. To have calculated angle in high preciseness, mechanical joints between the resistor and driven shaft as well as linear relationship between calculated angle of the driven shaft and output voltage of the goniometer were modified.

2.7. *Experimental procedure*

2.7.1. *Raw materials*

Three grain types, including wheat (Shiroudi variety), paddy (Kamfirouzi variety), and barley (Eram variety), commonly grown and consumed in Fars region, were obtained from Seed and Plant Breeding Unit, Agricultural Research Center of Fars province, Iran. Prior to trials, the seeds were cleaned by hand, removing mixed material such as stone, dust, and broken seeds. Some physical properties of the cleaned seeds were then determined.

2.7.2. *Physical properties*

To determine some physical properties of the seeds, 100 samples of each grain were randomly chosen. Three principal dimensions (length, width, and thickness) were then measured using a digital caliper (company: Neiko, state: New Jersey, country: USA, model: 01409A) reading to an accuracy of 0.02 mm. The samples were weighed with a precision electronic balance (company: A&D, city: Tokyo, country: Japan, model: GF-600) with 0.001 g accuracy. Additionally, some shape parameters of the samples (geometric mean diameter,

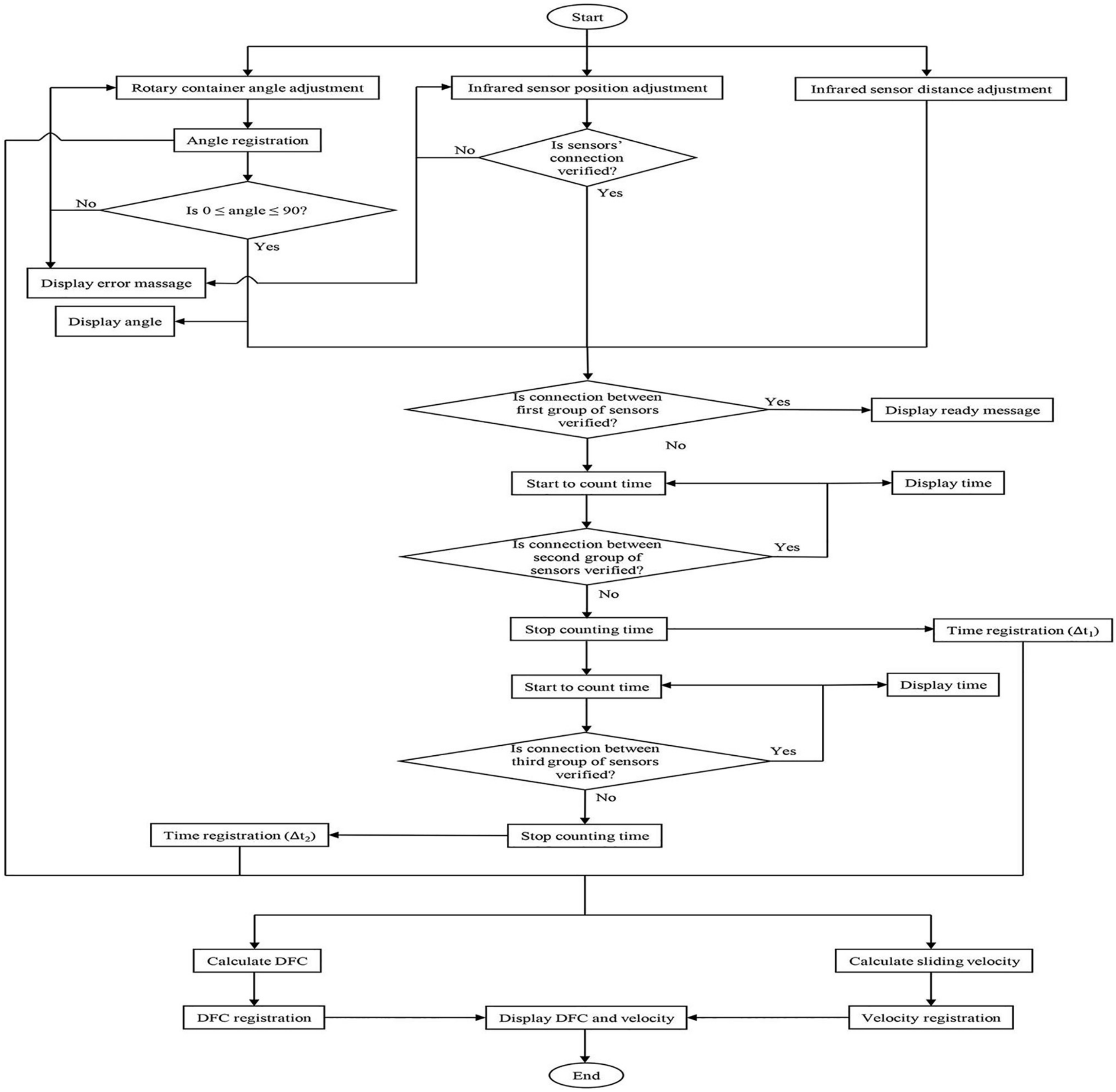

Fig. 7 – Operational flowchart of the DFC measuring system.

sphericity, and surface area) were respectively calculated using the following equations [52].

$$D_g = (LWT)^{1/3} \tag{16}$$

$$S = \left(\frac{D_g}{L}\right) \times 100 \tag{17}$$

$$S_a = \pi (D_g)^2 \tag{18}$$

2.7.3. *Determination of initial moisture content*

The initial moisture content of paddy grain was determined by drying 10 g of samples in a convection oven at 105 ± 2 °C until a constant weight was gained [53]. It was also carried out in case of wheat and barley grains through drying in a convection oven at 130 ± 1 °C for 19 and 20 h, respectively [54]. In order to avoid measurement error, all experiments were carried out triplicate and mean values were used. The initial moisture content of wheat, paddy, and barely grains was found to be 9.4, 7.3 and 8.2% d.b., respectively.

2.7.4. *Sample preparation*

The samples were packed in separate polyethylene bags and kept in a refrigerator at 5 ± 0.5 °C for ten days. Two hours before experiments, required quantity of the samples was placed at room temperature [55].

2.7.5. *Apparatus performance validation*

To appraise the apparatus performance, the SFC and DFC of the grains on five contact surfaces (aluminum, rubber,

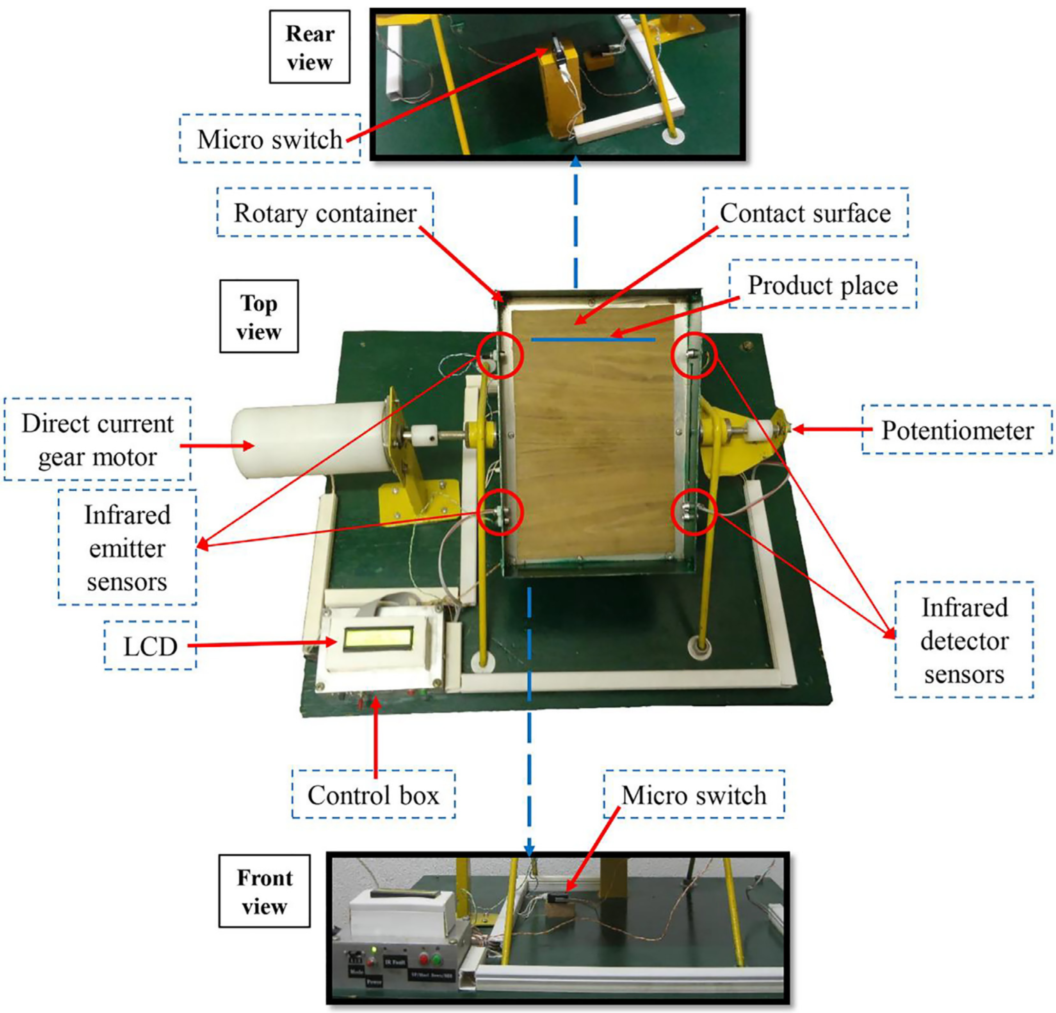

Fig. 8 – The fabricated friction coefficient measuring apparatus with defined elements.

glass, galvanized steel, and plywood) were measured using the fabricated apparatus (Fig. 8). In case of the DFC, three sliding velocities of 0.7, 2.3, and 5.6 cm/s were also evaluated for each combination. Before starting new trials, the contact surface was cleaned by compressed air to remove any contamination and cutin remaining from previous trials. A frame, with negligible weight, was used to confine sample on the contact surface. There was no contact between frame and the contact surface. All trials were carried out in three replications resulting in a total of 45 and 135 trails for the SFC and DFC measuring, respectively. The measuring procedure was completed by the apparatus as described in Sections 2.4.1 and 2.4.2 for the SFC and DFC, respectively.

To validate measurements, all trials were carried out using both new developed apparatus (based on tilting plate method) and the apparatus initially proposed by Clark and Mcfarland [41] (based on pulling force method). This pulling force method based apparatus was frequently used by previous researchers [56,19,57]. Details of development and engineering considerations of the apparatus are fully provided in the literature.

2.8. Data processing

The results obtained from the tilting plate method based apparatus developed in this work were then compared with those of pulling force method based apparatus by means of some statistical descriptor parameters (mean, standard deviation, the MAPE, and correlation coefficient) as the following equations [58–60].

$$M = \frac{\sum_{i=1}^{i=n} FC_i}{n} \tag{19}$$

$$SD = \frac{\sqrt{\sum_{i=1}^{i=n} (FC_i - M)^2}}{n} \tag{20}$$

$$MAPE = \frac{100}{n} \sum_{i=1}^{i=n} \left(\frac{|FC_{meas,i} - FC_{ind,i}|}{FC_{ind,i}} \right) \tag{21}$$

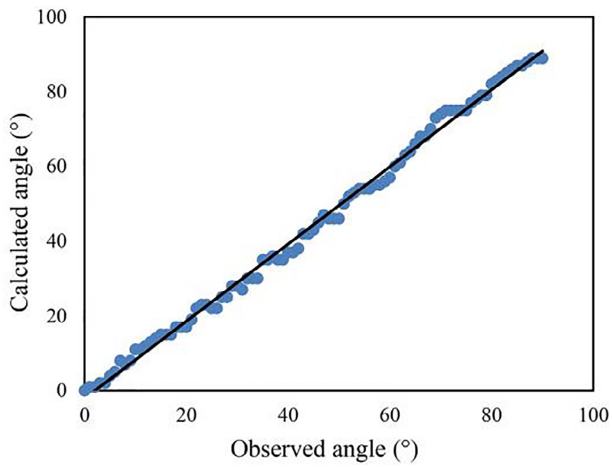

Fig. 9 – Relationship between calculated and observed angle values of rotary container.

3. Results and discussions

3.1. 1. Laboratory simulation

The prototype version of developed apparatus was confirmed in simulator setup in the laboratory. The simulation of each electrical element and unit in five appraised areas provided trustworthy results with satisfactory accuracy to meet user requirements for practical applications.

3.2. Calibration

The relation between calculated and observed angle values of rotary container is presented in Fig. 9. According to the Fig. 9, there was a good agreement between calculated and observed angle values with coefficient of determination of 0.996. Partial discrepancy might be due to use of mean angle values of calibration trails.

$$R = \frac{n\left(\sum_{i=1}^{i=n} FC_{meas,i} \times FC_{ind,i}\right) - \left(\sum_{i=1}^{i=n} FC_{meas,i}\right)\left(\sum_{i=1}^{i=n} FC_{ind,i}\right)}{\sqrt{\left[n\sum_{i=1}^{i=n}(FC_{meas,i})^2 - \left(\sum_{i=1}^{i=n} FC_{meas,i}\right)^2\right]\left[n\sum_{i=1}^{i=n}(FC_{ind,i})^2 - \left(\sum_{i=1}^{i=n} FC_{ind,i}\right)^2\right]}} \quad (22)$$

Moreover, to determine significant differences between performance of tilting plate method based apparatus and that of pulling force method based apparatus, the paired Student's t-test ($\alpha = 0.05$) was used and homogenous groups were then identified. The test was performed using SPSS 21 software (SPSS Inc., Chicago, IL, USA).

3.3. Physical properties

The mass, length, width, thickness, surface area, geometric mean diameter, and sphericity of the studied varieties of wheat, paddy, and barely grains are described in details in Table 3. Making comparison between data documented in

Table 3 – Some physical properties of the grains.

Physical property	Grain type	Mean	Standard deviation	Minimum	Maximum
Length (mm)	Wheat	7.131	1.104	6.513	8.658
	Paddy	8.152	0.862	7.123	9.641
	Barley	12.025	0.560	10.123	13.245
Width (mm)	Wheat	3.426	0.249	3.026	3.952
	Paddy	2.962	0.192	2.269	3.152
	Barley	2.745	0.253	2.004	3.121
Thickness (mm)	Wheat	2.526	0.156	2.251	2.791
	Paddy	1.770	0.103	1.352	2.025
	Barley	2.212	0.231	1.986	2.311
Mass (g)	Wheat	0.035	0.011	0.023	0.048
	Paddy	0.125	0.015	0.089	0.151
	Barley	0.037	0.009	0.031	0.042
Geometric mean diameter (mm)	Wheat	3.956	0.253	3.356	4.236
	Paddy	3.425	0.136	3.002	3.945
	Barley	4.259	0.330	3.123	4.564
Surface area (mm^2)	Wheat	49.105	1.023	47.921	51.650
	Paddy	32.652	2.569	27.123	37.134
	Barley	56.683	3.133	51.234	59.369
Sphericity (%)	Wheat	63.190	4.236	57.398	69.425
	Paddy	39.851	1.375	37.125	42.023
	Barley	32.123	1.368	29.131	34.523

Table 4 – Statistical descriptor parameters obtained for the SFC measurement by developed and typical apparatus.

Grain type	Measuring method	Type of contact surface				
		Aluminum	Rubber	Glass	Galvanized steel	Plywood
Wheat	Tilting plate	0.320 ± 0.061[a*]	0.495 ± 0.011[b**]	0.240 ± 0.009[c]	0.468 ± 0.031[d]	0.413 ± 0.007[e]
	Pulling force	0.329 ± 0.032[a]	0.485 ± 0.037[b]	0.237 ± 0.013[c]	0.475 ± 0.009[d]	0.422 ± 0.016[e]
Paddy	Tilting plate	0.236 ± 0.002[a]	0.513 ± 0.068[b]	0.135 ± 0.012[c]	0.405 ± 0.016[d]	0.395 ± 0.007[e]
	Pulling force	0.251 ± 0.022[a]	0.501 ± 0.026[b]	0.120 ± 0.009[c]	0.391 ± 0.028[d]	0.368 ± 0.051[e]
Barley	Tilting plate	0.212 ± 0.006[a]	0.410 ± 0.051[b]	0.182 ± 0.009[c]	0.398 ± 0.017[d]	0.326 ± 0.061[e]
	Pulling force	0.210 ± 0.011[a]	0.389 ± 0.007[b]	0.175 ± 0.021[c]	0.410 ± 0.008[d]	0.326 ± 0.025[e]

* The same letters for two measuring methods show insignificant differences at probability level of 5%.
** Mean ± standard deviation.

Table 5 – Statistical descriptor parameters obtained for the DFC measurement by developed and typical apparatus.

Grain type	Sliding velocity (cm/s)	Measuring method	Type of contact surface				
			Aluminum	Rubber	Glass	Galvanized steel	Plywood
Wheat	0.7	Tilting plate	0.212 ± 0.021[a*]	0.358 ± 0.025[b**]	0.126 ± 0.011[c]	0.258 ± 0.004[d]	0.306 ± 0.024[e]
		Pulling force	0.219 ± 0.006[a]	0.370 ± 0.017[b]	0.136 ± 0.003[c]	0.249 ± 0.021[d]	0.300 ± 0.014[e]
	2.3	Tilting plate	0.280 ± 0.013[a]	0.426 ± 0.016[b]	0.194 ± 0.002[c]	0.326 ± 0.024[d]	0.374 ± 0.013[e]
		Pulling force	0.286 ± 0.009[a]	0.441 ± 0.006[b]	0.207 ± 0.011[c]	0.313 ± 0.020[d]	0.388 ± 0.031[e]
	5.6	Tilting plate	0.335 ± 0.061[a]	0.481 ± 0.023[b]	0.249 ± 0.012[c]	0.381 ± 0.004[d]	0.429 ± 0.023[e]
		Pulling force	0.329 ± 0.023[a]	0.490 ± 0.011[b]	0.261 ± 0.007[c]	0.377 ± 0.011[d]	0.415 ± 0.033[e]
Paddy	0.7	Tilting plate	0.273 ± 0.020[a]	0.419 ± 0.013[b]	0.187 ± 0.012[c]	0.319 ± 0.024[d]	0.367 ± 0.013[e]
		Pulling force	0.259 ± 0.017[a]	0.404 ± 0.007[b]	0.176 ± 0.023[c]	0.312 ± 0.031[d]	0.350 ± 0.020[e]
	2.3	Tilting plate	0.341 ± 0.022[a]	0.487 ± 0.003[b]	0.255 ± 0.032[c]	0.387 ± 0.014[d]	0.435 ± 0.020[e]
		Pulling force	0.316 ± 0.037[a]	0.441 ± 0.031[b]	0.237 ± 0.018[c]	0.358 ± 0.021[d]	0.421 ± 0.027[e]
	5.6	Tilting plate	0.396 ± 0.012[a]	0.542 ± 0.013[b]	0.310 ± 0.022[c]	0.442 ± 0.013[d]	0.490 ± 0.011[e]
		Pulling force	0.369 ± 0.042[a]	0.512 ± 0.008[b]	0.300 ± 0.020[c]	0.409 ± 0.023[d]	0.465 ± 0.029[e]
Barley	0.7	Tilting plate	0.320 ± 0.007[a]	0.466 ± 0.006[b]	0.234 ± 0.016[c]	0.366 ± 0.011[d]	0.414 ± 0.017[e]
		Pulling force	0.339 ± 0.033[a]	0.478 ± 0.021[b]	0.212 ± 0.013[c]	0.385 ± 0.013[d]	0.392 ± 0.019[e]
	2.3	Tilting plate	0.388 ± 0.017[a]	0.534 ± 0.016[b]	0.302 ± 0.010[c]	0.434 ± 0.031[d]	0.482 ± 0.011[e]
		Pulling force	0.376 ± 0.021[a]	0.541 ± 0.011[b]	0.327 ± 0.010[c]	0.458 ± 0.023[d]	0.451 ± 0.029[e]
	5.6	Tilting plate	0.443 ± 0.025[a]	0.589 ± 0.011[b]	0.357 ± 0.016[c]	0.489 ± 0.011[d]	0.537 ± 0.032[e]
		Pulling force	0.469 ± 0.020[a]	0.552 ± 0.031[b]	0.330 ± 0.022[c]	0.459 ± 0.027[d]	0.565 ± 0.039[e]

* The same letters for two measuring methods show insignificant differences at probability level of 5%.
** Mean ± standard deviation.

the Table 3 and previous published data for the studied variety of wheat grain demonstrated that the obtained data variation range is in agreement with the results of studies denoted by Tabatabaeefar [23], Kalkan and Kara [61], and Markowski et al. [62] for other varieties of wheat grain. In case of the studied variety of paddy, obtained data variation range is in agreement with the results of studies reported by Reddy and Chakraverty [63] and Varnamkhasti et al. [64] for other varieties of paddy grain. Additionally, in case of the studied variety of barley, it was found that the obtained data variation range is in line with the results of studies published by Markowski et al. [65], Sologubik et al. [66], and Hamdani et al. [67] for other varieties of barley grain.

3.4. *Performance validation of developed apparatus*

Tables 4 and 5 indicate comparison of measurement of the SFC and DFC, respectively, by developed and typical apparatus for the studied grains. As it can be seen in the Tables 4 and 5, there was an excellent association, based on the paired Student's *t*-test ($\alpha = 0.05$), between obtained values of the newly developed tilting plate method based apparatus and those of the apparatus working based on pulling force method. Partial differences observed between the respective values might be due to use of mean values in conjunction with three measurement replications. Taking note from the Tables 4 and 5, it is found that maximum standard deviation for the SFC and DFC measured by the developed apparatus was 0.068 and 0.061, respectively.

According to the SFC and DFC manifested in the Tables 4 and 5, it can be stated that the SFC and DFC of the grains were different on contact surface of glass, aluminum, rubber, plywood, and galvanized steel. It is due to coarseness or smoothness of different contact surfaces. Smoother surface results in lower adhesion force between the grains and the surface and thereby, the lower SFC and DFC. With increasing surface roughness, deformation of surface asperities become relevant and therefore, the SFC and DFC increase [68,69]. This fact is described in more details by some authors [70,71]. They believed that synergistic interactions between asperities on the surface of agricultural product and those of the contact surface are effective in this phenomenon. With this in mind

Table 6 – Accuracy of the apparatus developed based on the tilting plate method.

Grain type	Type of friction coefficient	MAPE (%)	Correlation coefficient
Wheat	SFC	1.934	0.997
	DFC	3.443	0.993
Paddy	SFC	2.358	0.995
	DFC	4.986	0.996
Barley	SFC	2.963	0.998
	DFC	4.680	0.967

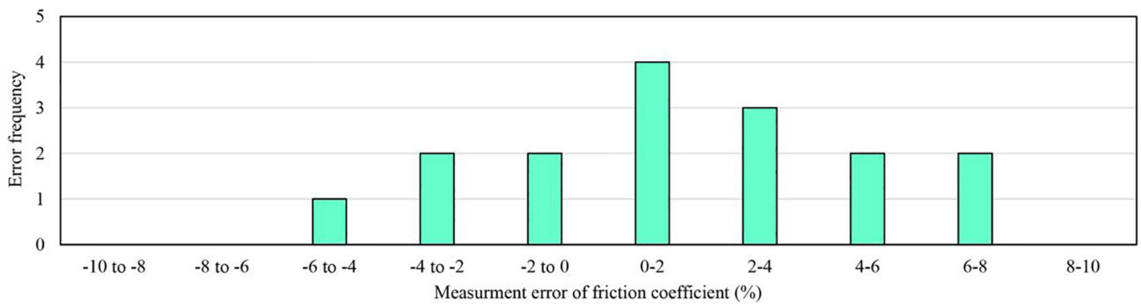

Fig. 10 – Frequency distribution of measurement error for the SFC.

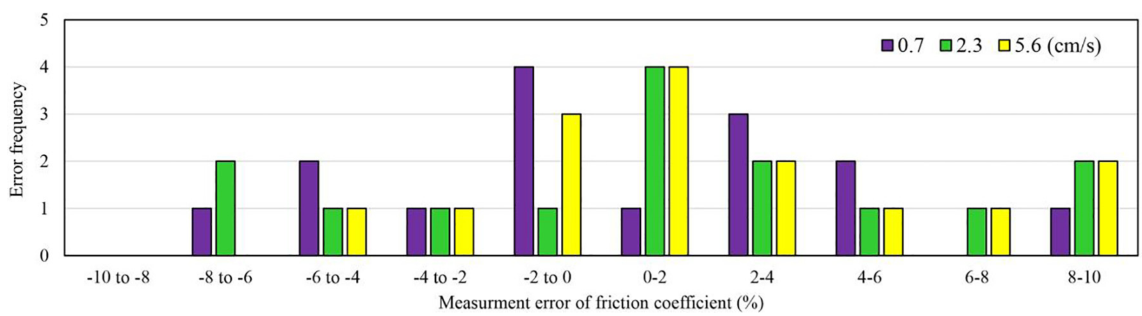

Fig. 11 – Frequency distribution of measurement error for the DFC.

that materials of contact surface are generally harder than biological materials of agricultural products, the contact surface asperities are not deformed within a short period of time. When an experimental surface contacts with an agricultural product, the asperities on the surface are embedded into the product surface and surface grooves are produced. The grooves cut fragments of biological material. Therefore, an increase in contact surface roughness increases the deformation component of friction force and consequently, the SFC and DFC increase. The positive effect of contact surface on the SFC and DFC has been issued for soybean [72] and popcorn kernel [73], respectively, which corresponds to the results of the present paper.

From the Table 5, it is also found that the DFC of the grains increased as sliding velocity increased. The reason behind this is explained by the fact that higher adhesive force at higher sliding velocity might result in the DFC growth [42]. The results of increasing effect of sliding velocity on the DFC of the grains in the current study were similar to those documented by Shafaei et al. [57] and Shafaei et al. [74] for pomegranate seeds and lavender flowers, respectively.

Accuracy of the apparatus developed in the study, obtained from comparison of measurement values from both tilting plate and pulling force methods, is reported in Table 6. According to the values in the Table 6, the correlation between two measuring methods was greater than 0.9 and the MAPE was less than 5% for all cases. Moreover, frequency distribution of measurement error for the SFC and DFC of the grains is graphically illustrated in Figs. 10 and 11, respectively. The statistical results indicated that the AAVME was 2.803 and 4.967% for measurement of the SFC and DFC, respectively. The MAVME was found to be 5.976 and 9.431% for measurement of the SFC and DFC, respectively.

To sum up validation of the integrated apparatus developed for accurate measurement of friction coefficients of agricultural products, it can be stated that the acceptable AAVME (<10%), MAVME (<10%), MAPE (<5%), and correlation coefficient (>0.9) imply high accuracy, stability, and efficiency of the developed apparatus for automatic measurements of the SFC and DFC. In other words, the new apparatus developed in this study based on tilting plate method was reliable enough to accurately measure both the SFC and DFC.

Table 7 – Comparison of the SFC and DFC of experimental grains measured by tilting plate method based apparatus, developed in this study, with previous published data.

Grain type	Type of friction coefficient	Measuring range	Reported range in literature	Measuring method used in literature	Authors
Wheat	SFC	0.240–0.495	0.210–0.713	Tilting plate, pulling force	Zhang et al. [75], Tabatabaeefar [23], Zaalouk and Zabady [76], Kaliniewicz [26], and Kaliniewicz et al. [28]
	DFC	0.126–0.490	0.163–0.875	Pulling force	Molenda et al. [6], Sharobeem [13], Asli-Ardeh et al. [50], Schwab [51], and Shafaei and Kamgar [60]
Paddy	SFC	0.135–0.513	0.223–0.590	Tilting plate, pulling force	Varnamkhasti et al. [77], Adebowale et al. [78], and Swaminathan and Guha [79]
	DFC	0.187–0.542	0.314–0.567	Rotating disk	Asli-Ardeh et al. [36]
Barley	SFC	0.182–0.410	0.116–0.993	Tilting plate, pulling force	Ozturk and Esen [80], and Kaliniewicz [26]
	DFC	0.234–0.589	–	–	–

3.5. *Comparison with published data*

A comparison of the SFC and DFC of the experimental grains obtained by the developed apparatus with previous published data is tabulated in Table 7. As it can be seen in the Table 7, the data measured in the present study are different from previously published data, although they are in the same range. These differences could be due to employment of various measuring methods (pulling force, tilting plate, and rotating disk). Another reason is attributed to various levels of moisture content and sliding velocity applied on the basis of desired experimental conditions. Moreover, it is corresponded to differences in contact surface type and the grain variety. However, surface asperities of contact surface and grain variety could be also different for the same type of contact surface and grain variety [71].

4. Conclusions and recommendations

In this study, an integrated mechatronic apparatus was developed based on tilting plate method for accurate measurement of the SFC and DFC of agricultural products. Generally, the apparatus is portable, compact, light weighted, simple, and includes inexpensive components. There is no need to modify hardware or software when it is applied for another agricultural product. Therefore, the developed apparatus has potential to be used for measuring the SFC and DFC of agricultural products.

The apparatus developed in this study is recommended to be used, as an assistive tool, by laboratory experts and researchers, and industrial users included but not limited in realms of Agricultural and Biosystems Engineering, and Food Science and Technology. The apparatus could be employed for accurate measurement of the SFC and DFC of agricultural products in case of experimental points, educational, demonstrational, and research targets. It is expected that, this development would result in a precise measurement of the SFC and DFC of agricultural products for optimization of design and performance of planting, harvesting, and post-harvest handling/processing machinery and equipment.

Acknowledgment

The authors are grateful to:

The financial support provided by the Scientific Society of Shiraz University under grant number of 13-93.

Anonymous respected reviewers who constructive comments have greatly aided in improving quality of the original manuscript.

Conflict of interest

We have no conflict of interest to declare.

REFERENCES

[1] ASAE. ASAE EP433 W/Corr. 1: Loads exerted by free-flowing grains on bins. ASABE, 2950 Niles Road, St. Joseph, MI 49085-9659, USA; 1988.

[2] Fluck RC, Wright FS, Splinter WE. Compression plunger, skinning and friction properties of sweet potatoes. Trans ASAE 1968;11(2):167–70.

[3] Stewart BR, Hossain QA, Kunze OR. Friction coefficients of sorghum grain on steel, teflon and concrete surfaces. Trans ASAE 1969;12(4):415–8.

[4] Schaper LA, Yaeger EC. Coefficients of friction of Irish potatoes. Trans ASAE 1992;35(5):1647–51.

[5] Puchalski C, Brusewitz GH. Coefficient of friction of watermelon. Trans ASAE 1996;39(2):589–94.

[6] Molenda M, Thompson SA, Ross IJ. Friction of wheat on corrugated and smooth galvanized steel surfaces. J Agr Eng Res 2000;77(2):209–19.

[7] Puchalski C, Brusewitz GH. Fruit ripeness and temperature affect friction coefficient of McLemore and Gala apples. Int Agrophys 2001;15(2):109–14.

[8] Molenda M, Horabik J, Ross IJ, Montross MD. Friction of wheat: grain-on-grain and on corrugated steel. Trans ASAE 2002;45(2):415–20.
[9] Puchalski C, Brusewitz GH, Dobrzanski JRB, Rybczynski R. Relative humidity and wetting affect friction between apple and flat surfaces. Int Agrophys 2002;16(1):67–71.
[10] Singh KK, Reddy BS, Varshney AC, Mangraj S. Physical and frictional of properties of orange and sweet lemon. Appl Eng Agric 2004;20(6):821–5.
[11] Altuntas E, Demirtola H. Effect of moisture content on physical properties of some grain legume seeds. New Zeal J Crop Hort 2007;35(4):423–33.
[12] Rusinek R, Molenda M. Static and kinetic friction of rapessed. Res Agr Eng 2007;53(1):14–9.
[13] Sharobeem YF. Apparent dynamic friction coefficients for grain crops. Misr J Ag Eng 2007;24(3):557–74.
[14] Subramanian S, Viswanathan R. Bulk density and friction coefficients of selected minor millet grains and flours. J Food Eng 2007;81(1):118–26.
[15] Ince A, Vursavus KK. Effect of sliding speed, abrasion surface and normal load on coefficient of friction of grapefruit (*Citrus paradisi*). Philipp Agric Sci 2008;91(3):308–14.
[16] Nwakonobi TU, Onwualu AP. Effect of moisture content and structural surfaces on coefficient of friction of two Nigerian food grains: sorghum (*Sorghum bicolor*) and millet (*Pennisetum glaucum*). Agric Eng Int CIGR EJ Manuscript 1152: Volume XI 2009.
[17] Li Z, Li P, Liu J. Physical and mechanical properties of tomato fruits as related to robot's harvesting. J Food Eng 2011;103 (2):170–8.
[18] Alizadeh M, Minaei S. Effect of de-awning and moisture content on some frictional properties of paddy. J Food Process Eng 2012;35(3):471–82.
[19] Locurto GJ, Bucklin RA, Thompson SA, Abdel-Hadi AI, Walton OR. Soybean coefficients of friction for aluminum, glass, and acrylic surfaces. Appl Eng Agric 2014;30(2):285–9.
[20] Nyendu GC, Pflum S, Schumacher P, Bern CJ, Brumm TJ. Friction coefficients for dried distillers grains on eight structural surfaces. Appl Eng Agric 2014;30(4):673–8.
[21] Singh KK, Goswami TK. Physical properties of cumin seed. J Agr Eng Res 1996;64(2):93–8.
[22] Nimkar PM, Chattopadhyay PK. Some physical properties of green gram. J Agr Eng Res 2001;80(2):183–9.
[23] Tabatabaeefar A. Moisture-dependent physical properties of wheat. Int Agrophys 2003;17(4):207–11.
[24] Bart-Plange A, Addo A, Aveyire J, Tutu E. Friction coefficient of maize, cowpea and groundnuts on different structural surfaces. J Sci Technol 2007;27(1):142–9.
[25] Lorestani AN, Rabani RH, Khazaei Y. Design and construction of an automatic coefficient of friction measuring device. Agric Eng Int CIGR J 2012;14(1):120–4.
[26] Kaliniewicz Z. Analysis of frictional properties of cereal seeds. Afr J Agric Res 2013;8(45):5611–21.
[27] Shafaei SM, Heydari AR, Masoumi AA, Sadeghi M. Determining and modeling of static friction coefficient of some agricultural seeds. Jordan J Agr Sci 2015;11(4):1007–19.
[28] Kaliniewicz Z, Anders A, Markowski P, Jadwisienczak K, Rawa T. Influence of cereal seed orientation on external friction coefficients. Trans ASABE 2016;59(3):1073–81.
[29] Chung JH, Verma LR. Determination of friction coefficients of beans and peanuts. Trans ASAE 1989;32(2):745–50.
[30] Shinners KJ, Koegel RG, Lehman LL. Friction coefficient of alfalfa. Trans ASAE 1991;34(1):33–7.
[31] Gupta RK, Das SK. Friction coefficients of sunflower seed and kernel on various structural surfaces. J Agr Eng Res 1998;71 (2):175–80.
[32] Henderson JM. Measuring kinetic friction coefficients using oscillatory motion. Trans ASAE 1967;10(3):348–51.
[33] Rademacher FJC. Accurate measurement of the kinetic coefficient of friction between a surface and a granular mass. Powder Technol 1978;19(1):65–77.
[34] Lawton PJ. Coefficients of friction between cereal grain and various silo wall materials. J Agric Eng Res 1980;25(1):75–86.
[35] Tsang-Mui-Chung M, Verma LR, Wright ME. A device for friction measurement of grains. Trans ASAE 1984;27 (6):1938–41.
[36] Asli-Ardeh EA, Abbaspour-Gilandeh Y, Shojaei S. Determination of dynamic friction coefficient of paddy grains on different surfaces. Int Agrophys 2010;24(2):101–5.
[37] Bickert WG, Buelow FH. Kinetic friction of grains on surfaces. Trans ASAE 1966;9(1):129–31.
[38] Snyder LH, Roller WL, Hall GE. Coefficients of kinetic friction of wheat on various metal surfaces. Trans ASAE 1967;10 (3):411–3.
[39] Clark RL, Welch GB, Fox WR. Kinetic friction of cotton seeds as affected by several factors. Trans ASAE 1970;13(6):708–9.
[40] Chen P, Squire EF. An evaluation of the coefficient of friction and abrasion damage of oranges on various surfaces. Trans ASAE 1971;14(6):1092–4.
[41] Clark RL, Mcfarland HA. Granular materials friction apparatus. Trans ASAE 1973;16(6):1198–9.
[42] Thompson SA, Ross IJ. Compressibility and frictional coefficients of wheat. Trans ASAE 1983;26(4):1171–6.
[43] Moore DW, White GM, Ross IJ. Friction of wheat on corrugated metal surfaces. Trans ASAE 1984;27(6):1842–7.
[44] Irvine DA, Jayas DS, Britton MG, White NDG. Dynamic friction characteristics of bulk seeds against flat vertical surfaces. Trans ASAE 1992;35(2):665–9.
[45] Bucklin RA, Molenda M, Bridges TC, Ross IJ. Slip-stick frictional behavior of wheat on galvanized steel. Trans ASAE 1996;39(2):649–53.
[46] Tavakoli T, Kermani AM, Khazaei J. Effects of normal pressure, sliding velocity and moisture content of chickpeas on dynamic friction coefficient on steel surfaces. J Agr Sci Tech 2002;4(1–2):11–22.
[47] Mingjin Y, Ling Y, Peixiang H, Qingdong L. Experimental research on dynamic friction coefficient of coated rice seeds. Agric Mech Asia Afr Lat Am 2003;34(1):18–20.
[48] Ghonimy MI. Determination of apparent dynamic coefficients of friction in processing food materials under high pressure. Misr J Ag Eng 2007;24(4):940–55.
[49] Ibrahim MM. Determination of dynamic coefficient of friction for some materials for feed pellet under different values of pressure and temperature. Misr J Ag Eng 2008;25(4):1389–409.
[50] Asli-Ardeh EA, Zadeh HM, Abbaspour-Gilandeh Y. Determination of dynamic friction coefficient in common wheat varieties on different contact surfaces. Agric Eng Int CIGR J 2017;19(1):136–41.
[51] Schwab CV. Apparent coefficient of friction of wheat on denim. J Agric Saf Health 2017;23(3):175–81.
[52] Mohsenin NN. Physical properties of plant and animal materials. New York: Gordon and Breach Science Publisher; 1986.
[53] AOAC. Official methods of analysis of the AOAC (15th Edition.). Arlington, VA: Association of Official Analytical Chemists, Inc; 1990.
[54] ASAE. ASAE S352.2 FEB03, Moisture Measurement-Unground Grain and Seeds. ASABE, 2950 Niles Road, St. Joseph, MI 49085-9659, USA; 2006.
[55] Abalone R, Cassinera A, Gaston A, Lara MA. Some physical properties of amaranth seeds. Biosyst Eng 2004;89(1):109–17.
[56] Thompson SA, Bucklin RA, Batich CD, Ross IJ. Variation in the apparent coefficient of friction of wheat on galvanized steel. Trans ASAE 1988;31(5):1518–24.
[57] Shafaei SM, Nourmohamadi-Moghadami A, Kamgar S. Analytical study of friction coefficients of pomegranate seed

as essential parameters in design of post-harvest equipment. Info Proc Agri 2016;3(3):133–45.
[58] Shafaei SM, Masoumi AA, Roshan H. Analysis of water absorption of bean and chickpea during soaking using Peleg model. J Saudi Soc Agric Sci 2016;15(2):135–44.
[59] Shafaei SM, Nourmohamadi-Moghadami A, Kamgar S. Development of artificial intelligence based systems for prediction of hydration characteristics of wheat. Comput Electron Agric 2016;128(1):34–45.
[60] Shafaei SM, Kamgar S. A comprehensive investigation on static and dynamic friction coefficients of wheat grain with the adoption of statistical analysis. J Adv Res 2017;8(4):351–61.
[61] Kalkan F, Kara M. Handling, frictional and technological properties of wheat as affected by moisture content and cultivar. Powder Technol 2011;213(1–3):116–22.
[62] Markowski M, Zuk-Gołaszewska K, Kwiatkowski D. Influence of variety on selected physical and mechanical properties of wheat. Ind Crops Prod 2013;47(1):113–7.
[63] Reddy BS, Chakraverty A. Physical properties of raw and parboiled paddy. Biosyst Eng 2004;88(4):461–6.
[64] Varnamkhasti MG, Mobli H, Jafari A, Keyhani AR. Soltanabadi MH, Rafiee S, Kheiralipour K. Some physical properties of rough rice (*Oryza Sativa* L.) grain. J Cereal Sci 2008;47(3):496–501.
[65] Markowski M, Majewska K, Kwiatkowski D, Malkowski M. Burdylo G. Selected geometric and mechanical properties of barley (*Hordeum Vulgare* L.) grain. Int J Food Prop 2010;13(4):890–903.
[66] Sologubik CA, Campanone LA, Pagano AM, Gely MC. Effect of moisture content on some physical properties of barley. Ind Crops Prod 2013;43(1):762–7.
[67] Hamdani A, Rather SA, Shah A, Gani A, Wani SM, Masoodi FA, et al. Physical properties of barley and oats cultivars grown in high altitude Himalayan regions of India. J Food Meas Charact 2014;8(4):296–304.
[68] Molenda M, Horabik J. Mechanical properties of granular agro-materials and food powders for industrial practice. Part I: characterization of mechanical properties of particulate solids for storage and handling. Institute of Agrophysics PAS, Lublin; 2005.
[69] Wiacek J, Molenda M, Horabik J. Mechanical properties of granular agro-materials. Continuum and discrete approach. Lublin: Institute of Agrophysics PAS; 2011.
[70] Kaliniewicz Z, Zuk Z. A relationship between friction plate roughness and the external friction angle of wheat kernels. Int J Food Prop 2017;20(3):2409–17.
[71] Kaliniewicz Z, Zuk Z, Krzysiak Z. Influence of steel plate roughness on the frictional properties of cereal kernels. Sustainability 2018;10(4):1–11.
[72] Kibar H, Ozturk T. Physical and mechanical properties of soybean. Int Agrophys 2008;22(3):239–44.
[73] Kalkan F, Kara M, Bastaban S, Turgut N. Strength and frictional properties of popcorn kernel as affected by moisture content. Int J Food Prop 2011;14(6):1197–207.
[74] Shafaei SM, Nourmohamadi-Moghadami A, Kamgar S. Experimental analysis and modeling of frictional behavior of lavender flowers (*Lavandula stoechas* L.). J Appl Res Med Aromat Plants 2017;4(1):5–11.
[75] Zhang Q, Puri VM, Manbeck HB. Model for frictional behavior of wheat on structural materials. Trans ASAE 1988;31(3):898–903.
[76] Zaalouk AK, Zabady FI. Effect of moisture content on angle of repose and friction coefficient of wheat grain. Misr J Agr Eng 2009;26(1):418–27.
[77] Varnamkhasti MG, Mobli H, Jafari A, Rafiee S, Heidarisoltanabadi M, Kheiralipour K. Some engineering properties of paddy (var Sazandegi). Int J Agr Biol 2007;9(5):763–6.
[78] Adebowale AA, Sanni LO, Owo HO, Karim OR. Effect of variety and moisture content on some engineering properties of paddy rice. J Food Sci Technol 2011;48(5):551–9.
[79] Swaminathan I, Guha M. Physical and engineering properties of some Indian paddy cultivars and their interrelations. Int J Engg Res Sci Tech 2016;5(3):136–43.
[80] Ozturk T, Esen B. Physical and mechanical properties of barley. Agric Tropica Subtrop 2008;41(3):116–21.